

Stability of the d -wave pairing with respect to the intersite Coulomb repulsion in cuprate superconductors

V. V. Val'kov^a, D. M. Dzebisashvili^a, M. M. Korovushkin^a, A. F. Barabanov^b

^aKirensky Institute of Physics, Federal Research Center KSC SB RAS, 660036 Krasnoyarsk, Russia

^bVereshchagin Institute for High Pressure Physics, 108840 Troitsk, Russia

Within the spin-fermion model for cuprate superconductors, the influence of the intersite Coulomb interactions V_2 and V'_2 between holes located at the next-nearest-neighbor oxygen ions of CuO_2 plane on the implementation of the $d_{x^2-y^2}$ -wave pairing is studied. It is shown that d -wave pairing can be suppressed only for unphysically large values of V_2 and V'_2 .

1. INTRODUCTION

It is known that the real structure of CuO_2 plane is characterized by the spatial separation of the subsystem of holes located at oxygen ions and the subsystem of spins localized at copper ions (Fig. 1). Besides, a number of features is caused by the presence of two oxygen ions in the unit cell of copper-oxygen plane. The minimal realistic microscopic model for cuprates is the three-band $p-d$ model (the Emery model) [1, 2]. This model takes into account the $d_{x^2-y^2}$ -orbitals of copper ions and p_x - and p_y -orbitals of oxygen ions. However, along with the realism, the multiband character of the Emery model leads to cumbersome analysis of cuprates physics. That is why a number of studies in this direction is carried out in the framework of the Hubbard model and its effective low-energy variants, such as $t-J$ and $t-J^*$ models on the simple square lattice. In these models, the same fermions form the charge and the spin subsystems.

Along with the number of important results, such an approach has a serious disadvantage: the Cooper pairing of fermions caused by the kinematic [3], exchange [4, 5], and spin-fluctuation mechanisms considered in the Hubbard [6, 7], $t-J$ [4, 5], or $t-J^*$ [8, 9] models is suppressed by the intersite Coulomb repulsion V_1 of charge carriers located at the neighboring sites. This effect is most pronounced in the d channel [10] and the Cooper instability disappears completely at $V_1 \sim 1-2$ eV.

In our previous paper [11], it has been shown that, because of the two-orbital character of the subsystem of holes located at oxygen sites and the spatial separation of this subsystem from that of spins at copper ions, the superconducting phase in high- T_c cuprates is stable with respect to the strong Coulomb repulsion of holes located at the nearest-neighbor oxygen sites if the order parameter has the $d_{x^2-y^2}$ -symmetry. This effect is due to the symmetry properties of the Coulomb potential.

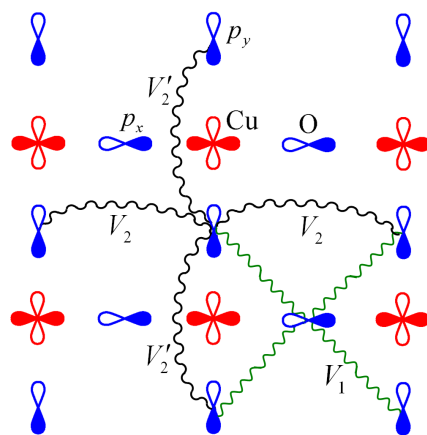


Fig. 1. Structure of CuO_2 plane. Here V_1 denotes the Coulomb interaction between holes located at the nearest-neighbor oxygen sites and V_2 and V'_2 correspond to the Coulomb interactions of holes located at the next-nearest-neighbor oxygen sites.

Note that in Ref. [11] the stability of the d -wave pairing was proved only for the case of the intersite Coulomb repulsion of holes located at the nearest-neighbor oxygen ions, V_1 , while the role of the Coulomb repulsion between holes located at the more distant oxygen ions, V_2 , is still unclear (the possibility of influence of V_2 on the superconducting d -wave pairing has been also mentioned in Ref. [12]). In this paper, we study the role of the Coulomb interaction between holes located at the next-nearest-neighbor oxygen ions on CuO_2 -plane in the implementation of the superconducting $d_{x^2-y^2}$ -wave pairing.

2. MODEL

In the strongly correlated regime, when the Hubbard repulsion energy U_d is large, i.e., $U_d > \Delta_{pd} \gg t_{pd}$, the $p-d$ model is reduced to the spin-fermion model [13, 14]

describing the subsystem of oxygen holes interacting with the spins located at copper ions. The Hamiltonian of the spin-fermion model is represented in the form

$$\begin{aligned}\hat{H} &= \hat{H}_0 + \hat{J} + \hat{I} + \hat{V}, \\ \hat{H}_0 &= \sum_{k\alpha} \left(\xi_0(k_x) a_{k\alpha}^\dagger a_{k\alpha} + \xi_0(k_y) b_{k\alpha}^\dagger b_{k\alpha} \right. \\ &\quad \left. + t_k (a_{k\alpha}^\dagger b_{k\alpha} + b_{k\alpha}^\dagger a_{k\alpha}) \right), \\ \hat{J} &= \frac{J}{N} \sum_{fkq\alpha\beta} e^{if(q-k)} u_{k\alpha}^\dagger (\mathbf{S}_f \boldsymbol{\sigma}_{\alpha\beta}) u_{q\beta}, \quad \hat{I} = \frac{I}{2} \sum_{\langle fm \rangle} \mathbf{S}_f \mathbf{S}_m, \\ \hat{V} &= V_2 \sum_f \hat{n}_{f+\frac{x}{2}} \hat{n}_{f+\frac{x}{2}+y} + V_2 \sum_f \hat{n}_{f+\frac{y}{2}} \hat{n}_{f+\frac{y}{2}+x} \\ &\quad + V_2' \sum_f \hat{n}_{f+\frac{x}{2}} \hat{n}_{f+\frac{x}{2}+x} + V_2' \sum_f \hat{n}_{f+\frac{y}{2}} \hat{n}_{f+\frac{y}{2}+y},\end{aligned}\quad (1)$$

where

$$\begin{aligned}\xi_0(k_{x(y)}) &= \varepsilon_p - \mu + \tau(1 - \cos k_{x(y)}), \\ t_k &= (2\tau - 4t) \sin \frac{k_x}{2} \sin \frac{k_y}{2}, \\ u_{k\beta} &= \sin \frac{k_x}{2} a_{k\beta} + \sin \frac{k_y}{2} b_{k\beta}, \\ \tau &= \frac{t_{pd}^2}{\Delta_{pd}} \left(1 - \frac{\Delta_{pd}}{U_d - \Delta_{pd} - 2V_{pd}} \right), \\ J &= \frac{4t_{pd}^2}{\Delta_{pd}} \left(1 + \frac{\Delta_{pd}}{U_d - \Delta_{pd} - 2V_{pd}} \right), \\ I &= \frac{4t_{pd}^4}{(\Delta_{pd} + V_{pd})^2} \left(\frac{1}{U_d} + \frac{2}{2\Delta_{pd} + U_p} \right).\end{aligned}\quad (3)$$

The Hamiltonian \hat{H}_0 describes the oxygen holes in the momentum representation. Here $a_{k\alpha}^\dagger$ ($a_{k\alpha}$) are the hole creation (annihilation) operators in the oxygen subsystem with the p_x -orbitals (Fig. 1), $\alpha = \pm 1/2$ is the spin projection. Similarly, $b_{k\alpha}^\dagger$ ($b_{k\alpha}$) are operators in the oxygen subsystem with the p_y -orbitals. The bare one-site energy of oxygen holes is ε_p , μ is the chemical potential, and t is the hopping integral. The operator \hat{J} describes the exchange interaction between the subsystem of oxygen holes and the subsystem of the spins localized at copper ions. Here, \mathbf{S}_f is the operator of a spin localized at site with index f and $\boldsymbol{\sigma} = (\sigma^x, \sigma^y, \sigma^z)$ is the vector of the Pauli matrices. The operator \hat{I} describes the superexchange interaction between the neighboring spins at copper ions. The intersite Coulomb interaction between holes is described by the operator \hat{V} . As far as the role of the Coulomb repulsion V_1 between holes located at the nearest oxygen sites was clarified in Ref. [11], here we do not take into account the corresponding term in the Hamiltonian \hat{V} and restrict ourselves to a treatment of the interactions V_2 and V_2' be-

tween the next-nearest neighbors (Fig. 1). In the Hamiltonian, $\hat{n}_{f+x(y)/2} = \sum_\sigma \hat{n}_{f+x(y)/2,\sigma}$ is the operator of the number of holes at the oxygen site $f+x(y)/2$, where $x = (1, 0)$ and $y = (0, 1)$ are the lattice basis vectors in the units of the lattice parameter.

When writing the Hamiltonian (1), we take into account that the hopping integrals in the first and the second terms can have different signs for different hopping directions owing to the different phases of the wave functions.

Below we use the commonly accepted set of parameters of the model: $t_{pd} = 1.3$ eV, $\Delta_{pd} = 3.6$ eV, $U_d = 10.5$ eV, $V_{pd} = 1.2$ eV [15–17]. Note that for this set, the parameter of the superexchange energy $I = 0.136$ eV (1570 K) agrees well with the experimental data on cuprate superconductors [17]. For the hopping integral of the holes, we use the value $t = 0.1$ eV [18], and we suppose that the parameters of the intersite Coulomb interactions are $V_2 = V_2' = 0.5 - 1.5$ eV.

It is important that the exchange energy between the localized and itinerant spins calculated using the expression (3) is large, namely, $J = 3.4$ eV $\gg \tau \approx 0.1$ eV. Therefore, to describe the oxygen holes dynamics it is necessary to take into account the exchange interaction rigorously. This problem is solved using the following basis set of operators [18, 19]

$$a_{k\alpha}, \quad b_{k\alpha}, \quad L_{k\alpha} = \frac{1}{N} \sum_{fq\beta} e^{if(q-k)} (\mathbf{S}_f \boldsymbol{\sigma}_{\alpha\beta}) u_{q\beta}, \quad (4)$$

where the third operator describes the strong spin-charge coupling.

3. EQUATIONS FOR GREEN'S FUNCTIONS

For consideration of the conditions for the Cooper instability, we supplement the basis set (4) by the operators ($\bar{\alpha} = -\alpha$)

$$a_{-k\bar{\alpha}}^\dagger, \quad b_{-k\bar{\alpha}}^\dagger, \quad L_{-k\bar{\alpha}}^\dagger. \quad (5)$$

The equations for the normal G_{ij} and the anomalous F_{ij} Green's functions obtained by the method [20, 21] can be represented in the form ($j = 1, 2, 3$)

$$\begin{aligned}(\omega - \xi_x)G_{1j} &= \delta_{1j} + t_k G_{2j} + J_x G_{3j} + \Delta_{1k} F_{1j}, \\ (\omega - \xi_y)G_{2j} &= \delta_{2j} + t_k G_{1j} + J_y G_{3j} + \Delta_{2k} F_{2j}, \\ (\omega - \xi_3)G_{3j} &= \delta_{3j} K_k + (J_x G_{1j} + J_y G_{2j}) K_k + \Delta_{3k} F_{3j}, \\ (\omega + \xi_x)F_{1j} &= \Delta_{1k}^* G_{1j} - t_k F_{2j} - J_x F_{3j}, \\ (\omega + \xi_y)F_{2j} &= \Delta_{2k}^* G_{2j} - t_k F_{1j} - J_y F_{3j}, \\ (\omega + \xi_L)F_{3j} &= \Delta_{3k}^* G_{3j} - (J_x F_{1j} + J_y F_{2j}) K_k.\end{aligned}\quad (6)$$

Here, $G_{11} = \langle\langle a_{k\uparrow}|a_{k\uparrow}^\dagger \rangle\rangle$, $G_{21} = \langle\langle b_{k\uparrow}|a_{k\uparrow}^\dagger \rangle\rangle$, and $G_{31} = \langle\langle L_{k\uparrow}|a_{k\uparrow}^\dagger \rangle\rangle$. The functions G_{i2} and G_{i3} are determined in a similar way with the only difference that $a_{k\uparrow}^\dagger$ is replaced by $b_{k\uparrow}^\dagger$ and $L_{k\uparrow}^\dagger$, respectively. The anomalous Green's functions are defined as $F_{11} = \langle\langle a_{-k\downarrow}^\dagger|a_{k\uparrow}^\dagger \rangle\rangle$, $F_{21} = \langle\langle b_{-k\downarrow}^\dagger|a_{k\uparrow}^\dagger \rangle\rangle$, $F_{31} = \langle\langle L_{-k\downarrow}^\dagger|a_{k\uparrow}^\dagger \rangle\rangle$. For F_{i2} and F_{i3} , the same type of notation regarding the second index is used. The functions involved in (6) are determined by the expressions

$$\begin{aligned} \xi_{x(y)} &= \xi_0(k_{x(y)}), \quad J_{x(y)} = J \sin \frac{k_{x(y)}}{2}, \quad K_k = \frac{3}{4} - C_1 \gamma_{1k}, \\ \xi_L(k) &= \varepsilon_p - \mu - 2t + 5\tau/2 - J \\ &+ [(\tau - 2t)(-C_1 \gamma_{1k} + C_2 \gamma_{2k}) + \tau(-C_1 \gamma_{1k} + C_3 \gamma_{3k})/2 \\ &+ J C_1(1 + 4\gamma_{1k})/4 - I C_1(\gamma_{1k} + 4)] K_k^{-1}. \end{aligned} \quad (7)$$

Here, γ_{jk} are the square lattice invariants: $\gamma_{1k} = (\cos k_x + \cos k_y)/2$, $\gamma_{2k} = \cos k_x \cos k_y$, $\gamma_{3k} = (\cos 2k_x + \cos 2k_y)/2$. In the course of deriving (6), we assume that the state of localized moments corresponds to the quantum spin liquid. Therefore, the spin correlation functions $C_j = \langle \mathbf{S}_0 \mathbf{S}_{r_j} \rangle$ satisfy the relations

$$C_j = 3 \langle S_0^x S_{r_j}^x \rangle = 3 \langle S_0^y S_{r_j}^y \rangle = 3 \langle S_0^z S_{r_j}^z \rangle, \quad (8)$$

where r_j is the position of a copper ion within the coordination sphere j . Besides, $\langle S_f^x \rangle = \langle S_f^y \rangle = \langle S_f^z \rangle = 0$.

From (6), it follows that the spectrum of the Fermi excitations in the normal phase is determined by the solution of the dispersion equation

$$\begin{aligned} \det_k(\omega) &= (\omega - \xi_x)(\omega - \xi_y)(\omega - \xi_L) - 2J_x J_y t_k K_k \\ &- (\omega - \xi_y) J_x^2 K_k - (\omega - \xi_x) J_y^2 K_k - (\omega - \xi_L) t_k^2 = 0. \end{aligned} \quad (9)$$

The spectrum is characterized by three bands ϵ_{1k} , ϵ_{2k} and ϵ_{3k} [22]. The branch ϵ_{1k} with the minimum at a point close to $(\pi/2, \pi/2)$ of the Brillouin zone arises owing to the strong spin-fermion coupling. At the low value of the number of holes per one oxygen ion n_p , the dynamics of holes is determined by the characteristics of the lower band ϵ_{1k} . This band is separated by an appreciable gap from the upper bands ϵ_{2k} and ϵ_{3k} [22].

The introduced order parameters $\Delta_{j,k}$ are related to the anomalous averages as follows

$$\begin{aligned} \Delta_{1k} &= -\frac{2}{N} \sum_q \left(V_2 \cos(k_y - q_y) \right. \\ &\quad \left. + V_2' \cos(k_x - q_x) \right) \langle a_{q\uparrow} a_{-q\downarrow} \rangle, \\ \Delta_{2k} &= -\frac{2}{N} \sum_q \left(V_2 \cos(k_x - q_x) \right. \\ &\quad \left. + V_2' \cos(k_y - q_y) \right) \langle b_{q\uparrow} b_{-q\downarrow} \rangle, \end{aligned}$$

$$\begin{aligned} \Delta_{3k} &= \frac{1}{N} \sum_q I_{k-q} \left\{ \langle L_{q\uparrow} L_{-q\downarrow} \rangle + C_{1x} \langle a_{q\uparrow} a_{-q\downarrow} \rangle \right. \\ &\quad \left. + C_{1y} \langle b_{q\uparrow} b_{-q\downarrow} \rangle + C_1 \psi_q (\langle a_{q\uparrow} b_{-q\downarrow} \rangle + \langle b_{q\uparrow} a_{-q\downarrow} \rangle) \right\} K_q^{-1} \\ &- \frac{1}{N} \sum_q \left\{ V_2 (C_1 \cos k_y - C_2 \gamma_{2k}) \cos q_y \right. \\ &\quad \left. + V_2' \left(-\frac{3}{8} + C_1 \cos k_x - \frac{C_3}{2} \cos 2k_x \right) \cos q_x \right\} K_q^{-1} \langle a_{q\uparrow} a_{-q\downarrow} \rangle \\ &- \frac{1}{N} \sum_q \left\{ V_2 (C_1 \cos k_x - C_2 \gamma_{2k}) \cos q_x \right. \\ &\quad \left. + V_2' \left(-\frac{3}{8} + C_1 \cos k_y - \frac{C_3}{2} \cos 2k_y \right) \cos q_y \right\} K_q^{-1} \langle b_{q\uparrow} b_{-q\downarrow} \rangle. \end{aligned} \quad (10)$$

Here $C_{1x(1y)} = C_1 \sin^2 \frac{q_{x(y)}}{2}$, $\psi_k = \sin \frac{k_x}{2} \sin \frac{k_y}{2}$ and $I_k = 4I \gamma_{1k}$.

4. EQUATIONS FOR THE SUPERCONDUCTING ORDER PARAMETERS

For the analysis of the conditions for the appearance of the Cooper instability, we express the anomalous Green's functions in terms of the Δ_{lk}^* parameters in the linear approximation

$$F_{nm}(k, \omega) = \sum_{l=1}^3 S_{nm}^{(l)}(k, \omega) \Delta_{lk}^* / \text{Det}_k(\omega), \quad (11)$$

where

$$\begin{aligned} \text{Det}_k(\omega) &= -\det_k(\omega) \det_k(-\omega), \\ S_{11}^{(1)}(k, \omega) &= Q_{3y}(k, \omega) Q_{3y}(k, -\omega), \\ S_{11}^{(2)}(k, \omega) &= S_{22}^{(1)}(k, \omega) = Q_3(k, \omega) Q_3(k, -\omega), \\ S_{33}^{(1)}(k, \omega) &= K_k S_{11}^{(3)}(k, \omega) = K_k^2 Q_y(k, \omega) Q_y(k, -\omega), \\ S_{22}^{(2)}(k, \omega) &= Q_{3x}(k, \omega) Q_{3x}(k, -\omega), \\ S_{33}^{(2)}(k, \omega) &= K_k S_{22}^{(3)}(k, \omega) = K_k^2 Q_x(k, \omega) Q_x(k, -\omega), \\ S_{12}^{(1)}(k, \omega) &= S_{21}^{(1)}(k, -\omega) = Q_3(k, \omega) Q_{3y}(k, -\omega), \\ S_{12}^{(2)}(k, \omega) &= S_{21}^{(2)}(k, -\omega) = Q_3(k, \omega) Q_{3x}(k, -\omega), \\ S_{12}^{(3)}(k, \omega) &= S_{21}^{(3)}(k, -\omega) = K_k Q_x(k, \omega) Q_y(k, -\omega), \\ S_{33}^{(3)}(k, \omega) &= K_k Q_{xy}(k, \omega) Q_{xy}(k, -\omega). \end{aligned} \quad (12)$$

The functions used here are

$$\begin{aligned} Q_{x(y)}(k, \omega) &= (\omega - \xi_{x(y)}) J_{y(x)} + t_k J_{x(y)}, \\ Q_3(k, \omega) &= (\omega - \xi_L) t_k + J_x J_y K_k, \\ Q_{3x(3y)}(k, \omega) &= (\omega - \xi_L)(\omega - \xi_{x(y)}) - J_{x(y)}^2 K_k, \\ Q_{xy}(k, \omega) &= (\omega - \xi_x)(\omega - \xi_y) - t_k^2. \end{aligned} \quad (13)$$

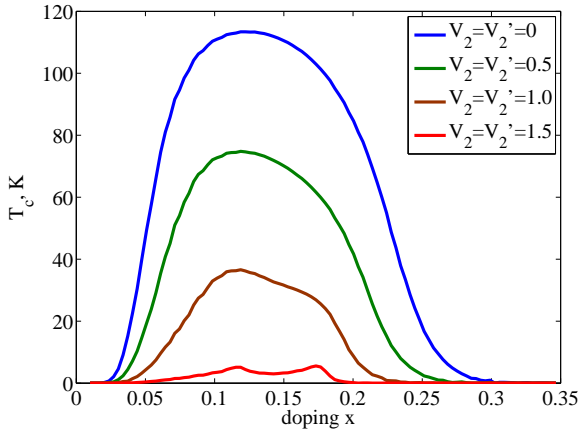


Fig. 2. Critical temperature for the transition to the superconducting $d_{x^2-y^2}$ phase versus doping at four values of the Coulomb repulsion parameter V_2 and V'_2 .

Using the spectral theorem [23], we find the expressions for the anomalous averages and finally arrive at the closed set of uniform integral equations for the superconducting order parameters ($l = 1, 2, 3$)

$$\begin{aligned}
\Delta_{1k}^* &= \frac{2}{N} \sum_{lq} (V_2 \cos(k_y - q_y) + V'_2 \cos(k_x - q_x)) M_{11}^{(l)}(q) \Delta_{lq}^* \\
\Delta_{2k}^* &= \frac{2}{N} \sum_{lq} (V_2 \cos(k_x - q_x) + V'_2 \cos(k_y - q_y)) M_{22}^{(l)}(q) \Delta_{lq}^* \\
\Delta_{3k}^* &= \frac{1}{N} \sum_{lq} \left\{ I_{k-q} \left[C_{1x} M_{11}^{(l)}(q) + C_{1y} M_{22}^{(l)}(q) - M_{33}^{(l)}(q) \right. \right. \\
&\quad \left. \left. + C_1 \phi_q (M_{12}^{(l)}(q) + M_{21}^{(l)}(q)) \right] \right. \\
&\quad \left. + \left[V_2 (C_1 \cos k_y - C_2 \gamma_{2k}) \cos q_y \right. \right. \\
&\quad \left. \left. + V'_2 \left(-\frac{3}{8} + C_1 \cos k_x - \frac{C_3}{2} \cos 2k_x \right) \cos q_x \right] M_{11}^{(l)}(q) \right. \\
&\quad \left. + \left[V_2 (C_1 \cos k_x - C_2 \gamma_{2k}) \cos q_x \right. \right. \\
&\quad \left. \left. + V'_2 \left(-\frac{3}{8} + C_1 \cos k_y - \frac{C_3}{2} \cos 2k_y \right) \cos q_y \right] M_{22}^{(l)}(q) \right\} \frac{\Delta_{lq}^*}{K_q}, \tag{14}
\end{aligned}$$

where

$$M_{nm}^{(l)}(q) = \frac{S_{nm}^{(l)}(q, E_{1q}) + S_{nm}^{(l)}(q, -E_{1q})}{4E_{1q}(E_{1q}^2 - E_{2q}^2)(E_{1q}^2 - E_{3q}^2)} \tanh\left(\frac{E_{1q}}{2T}\right).$$

Below, we use the system (14) to find the critical superconducting temperature.

In the Fig. 2, we illustrate the results obtained by solving Eq. 14 for the $d_{x^2-y^2}$ -wave pairing, where

$$\Delta_{lk} = \Delta_{l1} \cdot (\cos k_x - \cos k_y) + \Delta_{l2} \cdot (\cos 2k_x - \cos 2k_y).$$

One can see from Fig. 2 that an increase in V_2 and V'_2 leads to suppression of the d -wave pairing, however superconductivity is maintained up to unphysically large values $V_2 = V'_2 = 1.5$ eV of the Coulomb interaction between holes located at the next-nearest-neighbor oxygen ions (for comparison, the intensity of the Coulomb interaction between nearest-neighbor oxygen ions $V_1 = 1 - 2$ eV [16]).

CONCLUSION

To conclude, we have shown that the intersite Coulomb repulsion between holes located at the next-nearest-neighbor oxygen ions of CuO_2 plane suppresses the $d_{x^2-y^2}$ -wave pairing only at unphysically large values of the Coulomb interaction $V_2 = V'_2 = 1.5$ eV. Taking into account our previous result [11] on cancellation of the effect of the Coulomb interaction V_1 for the nearest-neighbor oxygen sites on the d -wave pairing, we conclude that an account for the real structure of CuO_2 plane leads to stability of the $d_{x^2-y^2}$ -wave pairing towards the strong intersite Coulomb repulsion. It is obvious that an account for the Coulomb interaction V_3 does not effect on the superconducting d -wave pairing because of the same "symmetry reason" as that for V_1 [11].

The work was supported by the Russian Foundation for Basic Research (RFBR) and partly by the Government of Krasnoyarsk Region (project nos. 16-42-240435 and 16-42-243057). The work of A.F.B. was supported by RFBR (project no. 16-02-00304). The work of M.M.K. was supported by grant of the President of the Russian Federation (project MK-1398.2017.2).

1. V. J. Emery, *Phys. Rev. Lett.* 58 (1987), p. 2794.
2. C. M. Varma, S. Schmitt-Rink and E. Abrahams, *Solid State Commun.* 62 (1987), p. 681.
3. R. O. Zaitsev and V. A. Ivanov, *Sov. Phys. Solid State* 29 (1987), p. 1475.
4. Yu. A. Izyumov, *Phys. Usp.* 40 (1997), p. 445; 42 (1999), p. 215.
5. N. M. Plakida, *High-Temperature Cuprate Superconductors*, Springer-Verlag, Berlin-Heidelberg (2010).
6. R. O. Zaitsev, *JETP* 98 (2004), p. 780.
7. V. V. Val'kov and M. M. Korovushkin, *JETP* 112 (2011), p. 108.
8. V. Yu. Yushankhai, G. M. Vujicic and R. B. Zakula, *Phys. Lett. A* 151 (1990), p. 254.
9. V. V. Val'kov, T. A. Val'kova, D. M. Dzebisashvili and S. G. Ovchinnikov, *JETP Lett.* 75 (2002), p. 378.
10. N. M. Plakida and V. S. Oudovenko, *Eur. Phys. J. B* 86 (2013), p. 115; *JETP* 146 (2014), p. 631.

11. V. V. Val'kov, D. M. Dzebisashvili, M. M. Korovushkin and A. F. Barabanov, *JETP Lett.* 103 (2016), p. 385.
12. N. M. Plakida, arXiv: 1607.02935.
13. A. F. Barabanov, L. A. Maksimov and G. V. Uimin, *JETP Lett.* 47 (1988), p. 622.
14. J. Zaanen and A. M. Oleś, *Phys. Rev. B.* 37 (1988), p. 9423.
15. M. S. Hybertsen, M. Schluter and N. E. Christensen, *Phys. Rev. B* 39 (1989), p. 9028.
16. M. H. Fischer and E.-A. Kim, *Phys. Rev. B* 84 (2011), p. 144502.
17. M. Ogata and H. Fukuyama, *Rep. Prog. Phys.* 71 (2008), p. 036501.
18. D. M. Dzebisashvili, V. V. Val'kov and A. F. Barabanov, *JETP Lett.* 98 (2013), p. 528.
19. V. V. Val'kov, D. M. Dzebisashvili and A. F. Barabanov, *JETP* 118 (2014), p. 959.
20. R. Zwanzig, *Phys. Rev.* 124 (1961), p. 983.
21. H. Mori, *Prog. Theor. Phys.* 33 (1965), p. 423.
22. V. V. Val'kov, D. M. Dzebisashvili and A. F. Barabanov, *Phys. Lett. A* 379 (2015), p. 421.
23. D. N. Zubarev, *Sov. Phys. Usp.* 3 (1960), p. 320.